

## Asymmetric electron angular distributions in resonant dissociative photoionization of $H_2$ with ultrashort xuv pulses

J. F. Pérez-Torres,<sup>1</sup> F. Morales,<sup>1</sup> J. L. Sanz-Vicario,<sup>2</sup> and F. Martín<sup>1</sup>

<sup>1</sup>*Departamento de Química C-9, Universidad Autónoma de Madrid, 28049 Madrid, Spain*

<sup>2</sup>*Grupo de Física Atómica y Molecular, Instituto de Física, Universidad de Antioquia, AA1226 Medellín, Colombia*

(Received 4 May 2009; published 22 July 2009)

Photoelectron angular distributions from fixed-in-space  $H_2$  molecules exposed to ultrashort xuv laser pulses have been evaluated. The theoretical method is based on the solution of the time-dependent Schrödinger equation in a basis of stationary states that include all electronic and vibrational degrees of freedom. Asymmetric angular distributions are observed as a consequence of the delayed ionization from the  $H_2$  doubly excited states, which induces interferences between gerade and ungerade ionization channels. The analysis of this asymmetry as a function of pulse duration can provide an estimate of the corresponding autoionization widths.

DOI: [10.1103/PhysRevA.80.011402](https://doi.org/10.1103/PhysRevA.80.011402)

PACS number(s): 33.20.Xx, 33.80.-b, 42.65.Re

Kinematically complete experiments, in which the momentum of all ejected electrons and atomic ions is determined in coincidence, have provided unprecedented insight on the dynamics of molecular photoionization [1–8]. In particular, they have opened the way to obtain fully differential photoelectron angular distributions (PADs) for specific energies of the ejected electrons or atomic ions and for well-defined orientations of the molecule with respect to the polarization direction of the incident radiation.

An important experimental effort has been devoted to study  $H_2$  ionization with synchrotron radiation [3,6,9–14] due to its simplicity and the possibility of comparing with accurate theoretical calculations [6,15,16]. A striking finding has been the observation of photoelectron angular distributions that do not respect the inversion symmetry of  $H_2$ . In Ref. [6], asymmetric angular distributions have been observed and theoretically predicted for linearly polarized light of 33 eV and  $H_2$  molecules oriented perpendicularly to the polarization direction. Evidence of a similar asymmetry was reported earlier for molecules oriented parallel to the polarization direction [3]. Calculations performed in the framework of stationary scattering theory have shown that the asymmetry only appears when molecular doubly excited states are efficiently populated [6]. This is because ionization channels in which the residual  $H_2^+$  ion is left in states of different inversion symmetry,  $1s\sigma_g$  and  $2p\sigma_u$ , interfere efficiently. In contrast, in the absence of doubly excited states, the electron angular distributions are perfectly symmetric [16]. It was then suggested [6,16] that the requirement for an efficient interference between  $g$  and  $u$  channels of the residual molecular ion could be the delayed ionization from the  $H_2$  doubly excited states.

To prove unambiguously that this is indeed the origin of the asymmetry, one has to follow the evolution of the photoelectron angular distribution with time. This is not a mere curiosity because, if true, one could use this strategy to estimate autoionization lifetimes. In this Rapid Communication we show that molecular autoionization lifetimes can be reasonably estimated by using ultrashort xuv pulses and by measuring the asymmetry of the photoelectron angular distributions as a function of pulse duration. This result applies to any homonuclear diatomic molecule in which ionization

leaves the remaining molecular ion in states with different inversion symmetry. Ultrashort xuv pulses are currently produced by high-order harmonic generation from gases exposed to intense infrared lasers. Thus, the combination of these radiation sources with multicoincidence detection techniques would be the obvious experimental approach to implement this idea. Such a strategy should be relevant to obtain autoionization lifetimes in more complex molecules.

In spite of the apparent simplicity of  $H_2$ , the study of ionization by using a time-dependent treatment is a formidable task. Autoionization is the result of electron correlation and, consequently, theoretical modeling must thus account for it. Furthermore, since  $H_2$  doubly excited states are dissociative and autoionization is slow, the nuclei have enough time to move outside the Franck-Condon (FC) region before the electron is effectively ejected (see Fig. 1). Therefore, the theory must also account for the nuclear motion. Finally, since direct ionization and autoionization interfere, a fully quantum mechanical treatment of both the electronic and

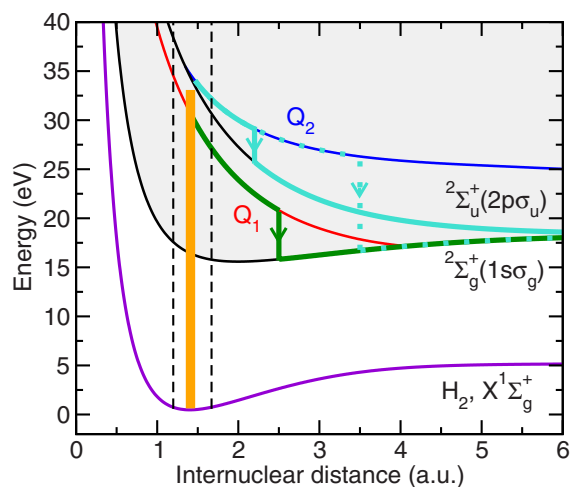


FIG. 1. (Color online) Potential-energy curves of  $H_2$  and  $H_2^+$ .  $Q_1$  denotes the lowest  $^1\Sigma_u^+$  doubly excited state above the  $1s\sigma_g$  threshold and  $Q_2$  denotes the lowest  $^1\Pi_u$  doubly excited state above the  $2p\sigma_u$  threshold. The thick vertical line illustrates absorption of a 33 eV photon. Semiclassical paths describing autoionization from the  $Q_1$  and  $Q_2$  states are also shown.

nuclear motions is required. A time-dependent theoretical method that fulfils the above requirements, i.e., that provides a quantum description of electrons and nuclei with inclusion of electron correlation in full dimensionality, has been recently proposed [17,18] and subsequently adapted to treat H<sub>2</sub> autoionization [19]. We have extended it here to account for the special boundary conditions associated with multicoincidence experiments.

Briefly, we have solved the time-dependent Schrödinger equation

$$\left[ \mathcal{H}^0(\mathbf{r}, R) + V(t) - i \frac{\partial}{\partial t} \right] \Phi(\mathbf{r}, R, t) = 0, \quad (1)$$

where  $\mathbf{r}$  represents the electronic coordinates  $\mathbf{r}_1$  and  $\mathbf{r}_2$ ,  $R$  is the internuclear distance,  $\mathcal{H}^0$  is the H<sub>2</sub> field-free nonrelativistic Hamiltonian,

$$\mathcal{H}^0(\mathbf{r}, R) = -\nabla_R^2/2\mu + \mathcal{H}_{el}(\mathbf{r}, R), \quad (2)$$

$\mathcal{H}_{el}$  is the electronic Hamiltonian, and  $V(t)$  is the laser-H<sub>2</sub> interaction potential in the dipole approximation

$$V(t) = \mathbf{p} \cdot \mathbf{A}_0 \sin^2(\pi t/T) \cos[\omega(t - T/2)], \quad (3)$$

$$0 \leq t \leq T = 0, \quad \text{elsewhere,}$$

with  $T$  as the pulse duration and  $\omega$  as the pulse frequency. In all calculations reported below we have considered a pulse with  $\omega = 33$  eV,  $T = 1-10$  fs, and  $I = A_0^2 \omega^2 = 10^{12}$  W/cm<sup>2</sup>. The time-dependent wave function  $\Phi(\mathbf{r}, R, t)$  is expanded in a basis of  $\sim 21\,000$  fully correlated vibronic stationary states of energy  $E_i$ ,  $\psi_i(\mathbf{r}, R)$ , which include the bound states, the nonresonant continuum states ( $\sim 19\,000$ ) and the doubly excited states of H<sub>2</sub> ( $\sim 1000$ ):

$$\Phi(\mathbf{r}, R, t) = \sum_i c_i(t) \psi_i(\mathbf{r}, R) \exp(-iE_i t). \quad (4)$$

The vibronic stationary states are written as products of an electronic wave function and a vibrational or dissociative wave function [18]. The former are obtained from configuration interaction calculations (for bound and doubly excited states) and  $L^2$  close-coupling calculations (for nonresonant continuum states) performed within a box and for a dense enough grid of internuclear distances [19]. Assuming the validity of the Born-Oppenheimer (BO) approximation, the  $\psi_i(\mathbf{r}, R)$  states are eigenstates of the field-free Hamiltonian at  $t = \infty$ . Thus, projection of  $\Phi(\mathbf{r}, R, t)$  onto the  $\psi_i(\mathbf{r}, R)$  states at  $t = \infty$  leads without any ambiguity to amplitudes that can be written in terms of the  $c_i$  expansion coefficients and can therefore be used to obtain the fully differential angular distributions in the usual way [16]. In a typical experiment in which the momentum of all ejected electrons and protons is detected in coincidence, angular distributions associated to the H+H<sup>+</sup> and H<sup>+</sup>+H dissociative ionization channels can be distinguished [20]. To properly account for these boundary conditions, the  $\Phi(\mathbf{r}, R, t)$  wave function must be projected onto stationary continuum states that localize one of the electrons in a given proton. At  $t \rightarrow \infty$ , the latter states are simply a linear combinations of the H<sub>2</sub><sup>+</sup> states associated with the  $1s\sigma_g$  and  $2p\sigma_u$  ionization channels. In practice, the system of

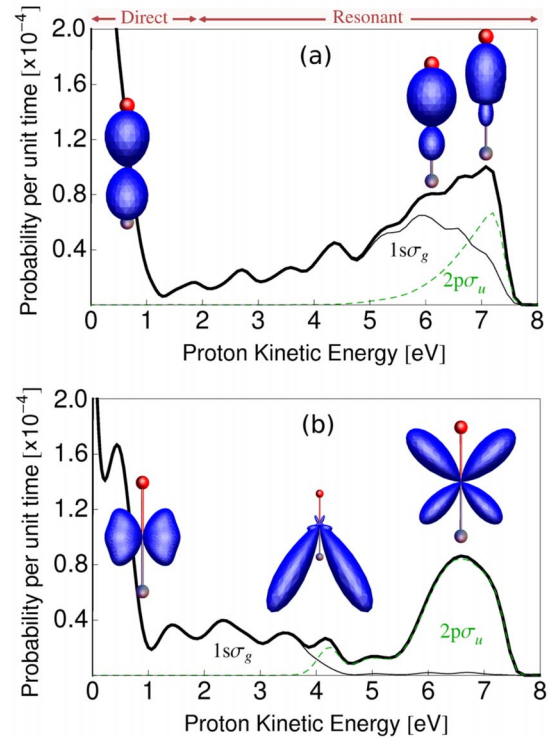


FIG. 2. (Color online) Proton kinetic-energy spectrum and photoelectron angular distributions for H<sub>2</sub> exposed to a xuv laser pulse of 33 eV, intensity of  $10^{12}$  W/cm<sup>2</sup>, and duration of 10 fs. H<sub>2</sub> is (a) parallel (final  $^1\Sigma_u^+$  symmetry) and (b) perpendicular (final  $^1\Pi_u$  symmetry) to the polarization direction. Thick solid line: ionization probability; thin solid line: contribution from the  $1s\sigma_g$  ionization channel; thin dashed line: contribution from the  $2p\sigma_u$  ionization channel. The angular distributions are shown for proton kinetic energies (a) 0.6, 6.1, and 7.1 eV and (b) 0.9, 4.1, and 6.6 eV. H<sup>+</sup> and H are indicated by red (upper) and gray (lower) balls, respectively.

coupled differential equation that arises upon substitution of expansion (4) into Eq. (2) is integrated up to  $t_{\max} \gg T$ ,  $1/\Gamma_r$ , where  $\Gamma_r$  is the autoionization width of the  $r$ th doubly excited state. Nonadiabatic couplings have been neglected. As a result of enclosing the system in a box, the continuum spectrum becomes discrete. To avoid artificial reflections of electrons and nuclei in the box boundaries, the energy spacing between discrete levels in both the electronic and dissociative continua must be smaller than the bandwidth of the pulse and the autoionization widths of the relevant doubly excited states.

Figure 2 shows the ionization probability as a function of the proton kinetic-energy release (KER) for a pulse of 10 fs and protons emitted at 0° and 90° with respect to the polarization vector. The figure also shows the PAD at three selected proton energies. For both orientations, the angular distributions are symmetric at very low KER ( $< 2$  eV). In this region, nonresonant ionization through the  $1s\sigma_g$  channel is by far the dominant process [21,22]. The asymmetry becomes apparent in the regions of the KER spectrum where (i) autoionization is the dominant process and (ii) the overlap between the  $1s\sigma_g$  and  $2p\sigma_u$  channels is significant. This confirms that the asymmetry of the PAD results from the inter-

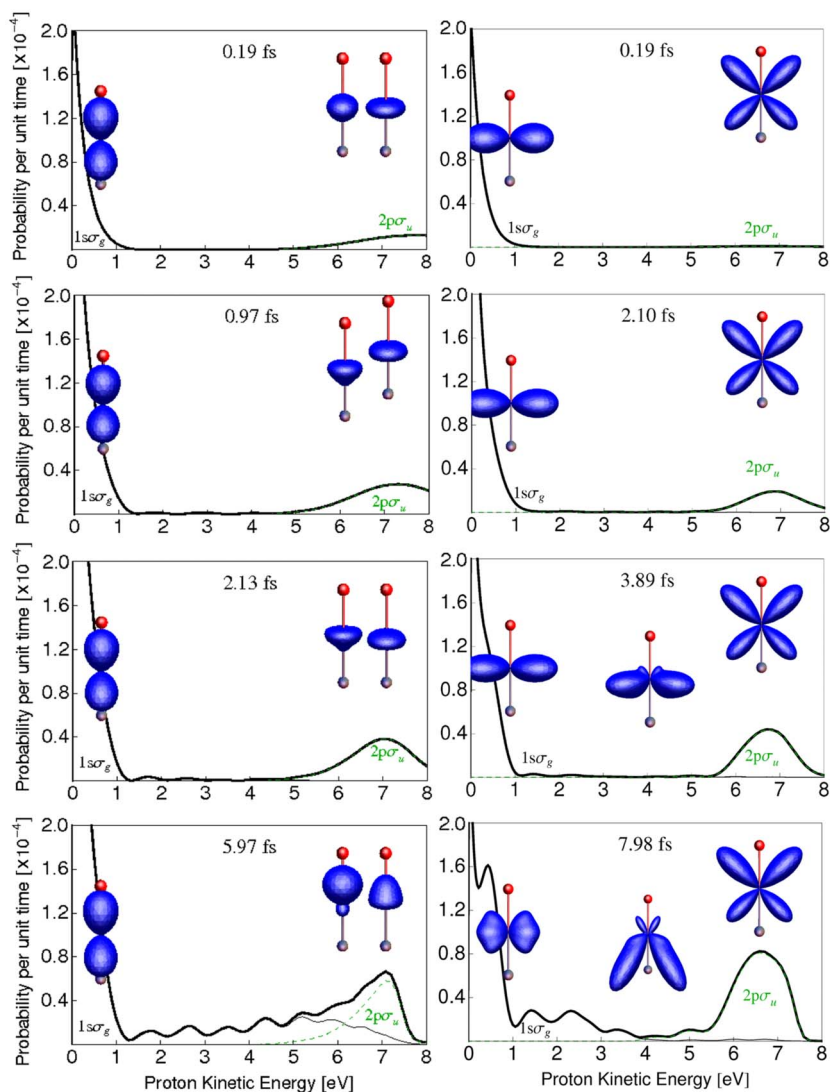


FIG. 3. (Color online) Time evolution of the proton kinetic-energy distribution and the photoelectron angular distributions for  $\text{H}_2$  exposed to a xuv laser pulse of 33 eV, intensity of  $10^{12}$  W/cm<sup>2</sup>, and duration of 10 fs. Left column: parallel orientation. Right column: perpendicular orientation. Angular distributions are only shown for probabilities that are significantly different from zero. Notations as in Fig. 2.

ference between ionization channels involving  $\text{H}_2^+$  states of different inversion symmetry [6]. The present results are very similar to those obtained with synchrotron radiation [6,16], thus indicating that all relevant physical processes induced by the radiation field occur in less than 10 fs. Nevertheless, some differences are apparent in KER regions of the order of the pulse bandwidth ( $\sim 0.8$  eV) in which the angular distributions vary rapidly with electron energy (e.g., at  $\sim 4$  eV for the parallel orientation).

To better understand the origin of the asymmetry, Fig. 3 shows the evolution of the KER spectra and the PADs with time. As can be seen, at very short times, the PADs are totally symmetric. In this case, only nonresonant ionization is possible, which leads to two peaks: one at low KER due to ionization through the  $1s\sigma_g$  channel and another one at high KER due to ionization through the  $2p\sigma_u$  channel. These peaks do not overlap because nonresonant ionization occurs exclusively in the FC region and the energy of the ejected electron (viz. the KER) is very different in each channel (see Fig. 1). Consequently, interference between these two channels is not possible. In the low KER region, the PAD remains symmetric forever because nonresonant ionization is always dominant [22,23]. However, as soon as autoionization ap-

pears in other regions of the KER spectrum and the electron energy becomes more similar in the  $1s\sigma_g$  and  $2p\sigma_u$  channels, the PAD becomes asymmetric because the latter two channels interfere. For the parallel orientation, the largest contribution to autoionization comes from the lowest  $Q_1$   $^1\Sigma_u^+$  doubly excited state, which can only decay through the  $1s\sigma_g$  channel; for the perpendicular orientation, it comes from the lowest  $Q_2$   $^1\Pi_u$  state, which can decay through both the  $1s\sigma_g$  and  $2p\sigma_u$  channels (at 33 eV, contribution from higher doubly excited is negligible). In the first case, the asymmetry results from the interference between autoionization through the  $1s\sigma_g$  channel and nonresonant ionization through  $2p\sigma_u$  channel, while, in the second case, it mainly results from the interference between the above two autoionization channels (see Fig. 1). It can be seen that the asymmetry is larger and develops faster in some regions of the KER spectrum than in others, which is due to the variation in the relative phase in the  $g$  and  $u$  channels and of the autoionization lifetime with internuclear distance. This evolution of the PADs with time shows that it is indeed the delayed ionization from the  $\text{H}_2$  doubly excited states that is responsible for the asymmetry of the PADs.

The above results suggest that measuring the asymmetry

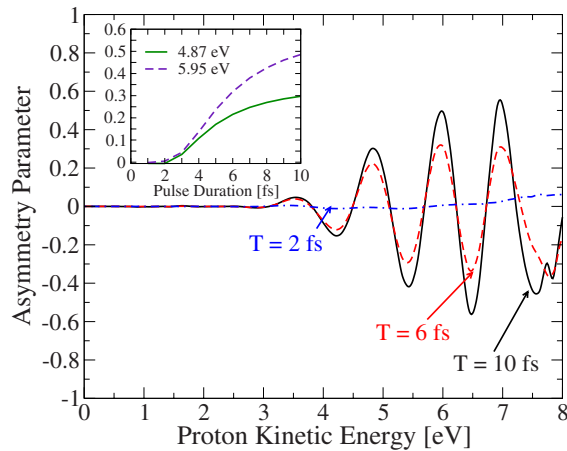


FIG. 4. (Color online) Asymmetry of the  $H_2$  photoelectron angular distribution versus proton kinetic energy for different pulse durations. The inset shows the variation in the asymmetry with pulse duration for a KER of 4.9 (full line) and 5.9 eV (dashed line).

of the PAD for different pulse durations can provide an estimate of the autoionization lifetimes. Figure 4 shows the asymmetry of the PAD in the parallel orientation as a function of KER for different pulse durations. The inset of the figure shows the variation in the asymmetry with the pulse duration for a specific KER. The asymmetry is defined as the normalized difference between the probabilities for an electron to escape in the direction of  $H^+$  or  $H$ . Thus it can only take values between  $-1$  and  $+1$ . For pulses longer than 10 fs, the asymmetry remains constant, thus indicating that one has reached the stationary regime. The magnitude of the asymmetry decreases as the pulse duration decreases. For a pulse duration of 2 fs, the asymmetry has practically disappeared, suggesting that there is no interference between the  $g$  and  $u$  ionization channels, i.e., between autoionization and direct ionization. This means that autoionization takes 2 fs and that, when it occurs, the pulse is no longer present to produce

direct ionization with which it can interfere. Hence, one can conclude that the lifetime of the lowest  $Q_1 \ ^1\Sigma_u^+$  doubly excited state should be  $\sim 2$  fs. This is consistent with the average value of the autoionization width in the FC region [24,25]. The situation is quite different in the perpendicular case because autoionization from the  $Q_2$  states proceeds through both the  $1s\sigma_g$  and  $2p\sigma_u$  channels (see Fig. 1). Since the two channels are populated both during and after the pulse, they will always interfere irrespective of the pulse duration. Therefore, the asymmetry never disappears except if, by chance, the relative phase is such that it leads to no effective interference (as for the proton energies leading to nodes in Fig. 4). Hence the necessary condition to obtain symmetric angular distributions by reducing the pulse duration is that either the  $g$  or the  $u$  channel is mainly populated by direct ionization.

In conclusion, we have shown that the asymmetry in the photoelectron angular distributions produced in dissociative photoionization of  $H_2$  is due to the delayed ionization from doubly excited states. We have also shown that ultrashort xuv pulses can be used to estimate the autoionization lifetimes of the lowest doubly excited states by studying the variation in that asymmetry with pulse duration. Another, more involved, possibility would be to perform pump-probe experiments with a xuv pump pulse much shorter than 2 fs and a probe pulse that is delayed from the former in a controlled way. Which observables should be analyzed in this case is the subject of current investigations.

We thank Mare Nostrum BSC and CCC-UAM for allocation of computer time. This work was partially supported by the DGI Projects No. FIS2007-60064 and No. CSD2007-00010 and the European COST Action CM0702. J.L.S.-V. acknowledges financial support from Vicerrectoría de Investigación of Universidad de Antioquia and Colciencias agency, and J.F.P.-T. acknowledges the Alban Program for Latin-America Scholarship No. E07D401391CO.

- [1] J. Ullrich, R. Moshhammer, R. Dörner, O. Jagutzki, V. Mergel, H. Schmidt-Böcking, and L. Spielberger, *J. Phys. B* **30**, 2917 (1997).
- [2] T. Jahnke *et al.*, *Phys. Rev. Lett.* **88**, 073002 (2002).
- [3] A. Lafosse, M. Lebech, J. C. Brenot, P. M. Guyon, L. Spielberger, O. Jagutzki, J. C. Houver, and D. Dowek, *J. Phys. B* **36**, 4683 (2003).
- [4] T. Jahnke *et al.*, *Phys. Rev. Lett.* **93**, 083002 (2004).
- [5] J. Ullrich, R. Moshhammer, A. Dorn, R. Dörner, L. P. H. Schmidt, and H. Schmidt-Böcking, *Rep. Prog. Phys.* **66**, 1463 (2003).
- [6] F. Martín *et al.*, *Science* **315**, 629 (2007).
- [7] M. S. Schöffler *et al.*, *Science* **320**, 920 (2008).
- [8] B. Zimmermann *et al.*, *Nat. Phys.* **4**, 649 (2008).
- [9] Th. Weber *et al.*, *Nature (London)* **431**, 437 (2004).
- [10] Th. Weber *et al.*, *Phys. Rev. Lett.* **92**, 163001 (2004).
- [11] M. Gisselbrecht *et al.*, *Phys. Rev. Lett.* **96**, 153002 (2006).
- [12] D. Akoury *et al.*, *Science* **318**, 949 (2007).
- [13] K. Kreidi *et al.*, *Phys. Rev. Lett.* **100**, 133005 (2008).
- [14] T. J. Reddish, J. Colgan, P. Bolognesi, L. Avaldi, M. Gisselbrecht, M. Lavollée, M. S. Pindzola, and A. Huetz, *Phys. Rev. Lett.* **100**, 193001 (2008).
- [15] F. Martín, *J. Phys. B* **32**, R197 (1999).
- [16] J. Fernández and F. Martín, *New J. Phys.* **11**, 043020 (2009).
- [17] A. Palacios, H. Bachau, and F. Martín, *Phys. Rev. Lett.* **96**, 143001 (2006).
- [18] A. Palacios, H. Bachau, and F. Martín, *Phys. Rev. A* **74**, 031402(R) (2006).
- [19] J. L. Sanz-Vicario, H. Bachau, and F. Martín, *Phys. Rev. A* **73**, 033410 (2006).
- [20] Experiments that do not distinguish between the  $H+H^+$  and  $H^++H$  channels always lead to symmetric electron angular distributions.
- [21] K. Ito, R. I. Hall, and M. Ukai, *J. Chem. Phys.* **104**, 8449 (1996).
- [22] I. Sánchez and F. Martín, *Phys. Rev. Lett.* **82**, 3775 (1999).
- [23] I. Sánchez and F. Martín, *Phys. Rev. Lett.* **79**, 1654 (1997).
- [24] J. Tennyson, *At. Data Nucl. Data Tables* **64**, 253 (1996).
- [25] I. Sánchez and F. Martín, *J. Chem. Phys.* **106**, 7720 (1997).